Journal of Alloys and Compounds 578 (2013) 553–558

Contents lists available at SciVerse ScienceDirect

Journal of Alloys and Compounds

journal homepage: www.elsevier.com/locate/jalcom

Zirconium alloys produced by recycling zircaloy tunings

N.S. Gamba [a], I.A. Carbajal-Ramos [b], M.A. Ulla [a], B.T. Pierini [a], F.C. Gennari [b,*]

[a] Instituto de Investigaciones en Catálisis y Petroquímica, INCAPE (FIQ, UNL–CONICET), Santiago del Estero 2829, 3000 Santa Fe, Argentina
[b] Centro Atómico Bariloche, CNEA e Instituto Balseiro, Universidad Nacional de Cuyo, Av. Bustillo 9500, 8400 Bariloche, Argentina

ARTICLE INFO

Article history:
Received 20 May 2013
Received in revised form 24 June 2013
Accepted 2 July 2013
Available online 10 July 2013

Keywords:
Hydrides
Zirconium
Titanium
Mechanical milling
Zircaloy

ABSTRACT

Zircaloy chips were recycled to successfully produce Zr–Ti alloys with bcc structure and different compositions. The procedure developed involves two steps. First, the reactive mechanical alloying (RMA) of the zircaloy tunings and Ti powders was performed to produce metal hydride powders, with a high refinement of the microstructure and a Zr–Ti homogeneous composition. Second, the metal hydride powders were thermally decomposed by heating up to 900 °C to synthesize the Zr-based alloy with a selected composition. The change in the nature of the powders from ductile to brittle during milling avoids both cold working phenomena between the metals and the use of a control agent. A minimum milling time is necessary to produce the solid solution with the selected composition. The microstructure and structure of the final alloys obtained was studied. The present procedure could be extended to the production of Zr-based alloys with the addition of other metals different from Ti.

1. Introduction

Zirconium-based alloys are used in different applications such as aircraft, space devices, chemical and nuclear industries. Zirconium alloys exhibit high mechanical strength, high fracture toughness and good corrosion resistance [1]. In the last few years, Zr alloyed with Ti has demonstrated superior mechanical properties than pure Ti, excellent resistance to biologic fluids and good biocompatibility [2,3]. Therefore, Zr–Ti alloys have a high biomedical interest due to the adequate combination of properties.

Zr and Ti are known to have analogous structure and chemical properties. At ambient condition, both Zr and Ti crystallize in a hexagonal closed-packed (hcp) structure (α phase) [4]. At high temperatures of 863 and 882 °C, they transform into a body-centered cubic (bcc) β phase. The melting points of bcc Zr and Ti are 1852 °C and 1670 °C, respectively. Due to their similarities, Zr and Ti metals form a continuous series of solid solutions between the low temperature α phase (hcp) and the high temperature β phase (bcc). For the equiatomic ZrTi alloy, the α–β transition temperature has a minimum at about 605 °C [4]. Interestingly, a wide compositional variation of Zr–Ti alloy is available due to the complete solid solubility between Zr and Ti. In a recent work, Hsu et al. [5] studied the mechanical properties of a series of binary Zr–Ti alloys, with Zr contents up to 40 wt%. The results showed that when the concentration of Zr in the alloys increased, strength, elastic recovery angles and hardness also increased. Other contributions [6,7] evaluated mechanical properties and grindability of Ti by alloying with Zr (10–50 wt.%). The Ti–Zr alloy phases varied according to the composition and cooling conditions, with improved grindability for 40 wt.% of Zr [7,8]. On the other hand, the structure and mechanical properties of pure Zr and a series of binary Zr–Ti (10–40 wt.%) alloys was investigated as potential dental implant materials. Zr–Ti alloys exhibited low modulus, ductility, excellent elastic recovery capability and impressive strength [9].

In all these studies, Zr–Ti alloys were produced by melting Zr and Ti together and then re-melting several times prior to casting, in order to improve chemical homogeneity [5–9]. However, the fact that both Zr and Ti have high melting temperature and high reactivity with oxygen and impurities at elevated temperatures makes them difficult to melt [10]. In view of this, the mechanical alloying (MA) emerges as one of the most cost-adequate method to synthesize refined particles or nanoalloys with controlled composition and reduced reactivity with oxygen at room temperature [11]. In particular, reactive mechanical alloying (RMA) is an attractive method for the size reduction of coarse particles, which favors the alloying with other components and simultaneously induces the development of amorphous phases. The first attempt to prepare Zr–Ti nanocrystalline materials was made by Aoki et al. [12]. They performed RMA under nitrogen atmosphere at room temperature to produce fcc $ZrTiN_{0.9}$ or α-$ZrTiN_{0.3}$ powders, depending on nitrogen pressure. In a later work using different milling atmospheres (N_2, O_2 and H_2), these authors demonstrated that the amorphization of pure metals exhibiting complete solid solubility, such as Zr and Ti, is hard or practically impossible: the

* Corresponding author. Address: Instituto Balseiro (UNCuyo), Centro Atómico Bariloche (CNEA) and Consejo Nacional de Investigaciones Científicas y Técnicas (CONICET), Av. Bustillo 9500, R8402AGP S.C. de Bariloche, Argentina. Tel.: +54 2944 445118; fax: +54 2944 445190.
E-mail address: gennari@cab.cnea.gov.ar (F.C. Gennari).

0925-8388/$ - see front matter © 2013 Elsevier B.V. All rights reserved.
http://dx.doi.org/10.1016/j.jallcom.2013.07.025

final amorphous product contained the component of the atmosphere [13]. In a subsequent work, $Ti_{50}Zr_{50}$ nanocomposite was successfully produced by roller vibration milling at room temperature, using stearic acid as control agent [14]. However, part of Zr and Ti powders remain unreacted. The $Ti_{50}Zr_{50}$ composite remains hexagonal, but the axial ratio is smaller than that of the corresponding hcp structure. Looking for a Zr–Ti alloy with high porosity and high surface area for biomedical applications, Wen et al. [15] produced TiZr alloy foams by a combination of MA using stearic acid and powder metallurgical process (mixing with space-holding particles, compacting and heat treatment up to 1200 °C). The TiZr foams obtained have a bimodal porous structure, with macropores between 200 and 500 μm and micropores of several microns. In these previous studies [12–15], the starting materials were pure Zr and Ti sponges or powders.

Zircaloy tunings are generated in large quantities during the production of zircaloy tubes and rods for nuclear reactors [16]. These waste materials are a valuable source of Zr, with contents greater than 97.5% of Zr metal in zircaloy-4 and minor amounts of Sn (1.2–1.7%) and Fe + Cr (0.18–0.38%). Although the cost of recycled materials is lower than the cost of those produced by conventional methods, it is difficult to recycle the tunings due to their elongated spiral shape and small size in comparison with the scraps. In addition, their surface area is relatively large and they are covered with oxides and oil emulsion, so that their recycling through the remelting process is difficult. Therefore, a process for recovering pure Zr metal from zircaloy tunings is in practical demand.

In this work, we fabricate Zr alloys by RMA of zircaloy tunings and titanium powders followed by annealing at low temperature. Milling under hydrogen avoids cold working phenomena between Zr and Ti due to the change from ductile to brittle nature of the powders and facilitates the particle size refinement and alloying process. Posterior heating under argon atmosphere up to 900 °C produces Zr–Ti alloys with particular microstructural characteristics. The effect of the milling time on the structure and microstructure of the alloys obtained was studied.

2. Experimental

Zircaloy-4 tunings (Zry), whose nominal composition is Zr = 98.4–97.8 wt%; Sn = 1.2–1.7 wt%; Cr = 0.07–0.13 wt% and Fe = 0.18–0.24 wt%, and titanium powders (Aldrich, 99.9%) were used as starting materials. Zry tunings were first cleaned with detergent, washed with acetone to eliminate oil residues and finally dried in air. The shape and dimensions of Zry machine flakes are very variable, with widths of 0.1–0.3 cm and lengths of 1–5 cm (Fig. 1a). Fig. 1b shows spherical particles of Ti starting powders, which range from 25 to 150 μm. Mixtures of Zr (as main component of Zry, considering 98% Zr) and Ti with 1:1 and 1:2 ratios together with ferromagnetic steel balls were placed in a stainless steel container and enclosed in an argon dry box (oxygen and moisture <5 ppm). These mixtures were referred to as Zr–Ti and Zr–2Ti for 1:1 and 1:2 compositions, respectively. Milling was carried out under argon or hydrogen atmosphere in a Uni-Ball-Mill II apparatus (Australian Scientific Instrument), with a ball to powder weight ratio of 53:1. The samples were milled from 1 h up to a maximum time of 30 h. At regular intervals, small amounts of powder were taken out for analysis. When milling was performed under hydrogen atmosphere, the mill container was evacuated prior to filling with high purity hydrogen gas (0.5 MPa) and this operation was repeated several times to avoid oxygen contamination. As milling time progresses, the container was systematically refilled in order to keep the hydrogen pressure constant.

Hydriding experiments on Zry tunings and Ti powders were conducted under non–isothermal conditions from 20 to 400 °C using a modified Sieverts–type device. The hydrogen pressure used for hydriding was 0.5 MPa with a constant heating rate of 5 °C. min^{-1}. These runs were performed to determine the hydriding onset temperature for each starting material.

Structural and microstructural changes were studied by X-ray Powder Diffraction (XRPD, Philips PW 1710/01 Instruments), using Cu Kα radiation and graphite monochromator. During the XRPD data collection all the samples were maintained under Ar atmosphere using a tightly sealed sample holder to prevent reaction with air. X-ray diffractograms were acquired using a step size of 0.02 and a counting time of 1.4 s. XRPD patterns of Zry tunings and Ti powders show diffraction peaks corresponding to the low temperature structure of Zr and Ti (hcp), respectively (not shown). No evidence of oxide layer was detected by XRPD, probably due to its thin and amorphous nature. Crystallite sizes of as-milled and as-heated powders were estimated from the most intense diffraction peak of each phase using the Scherrer equation. The correction of the instrumental broadening was made using standard silicon (Si) powder. The adjusted full width at half the maximum intensity was used in each calculation.

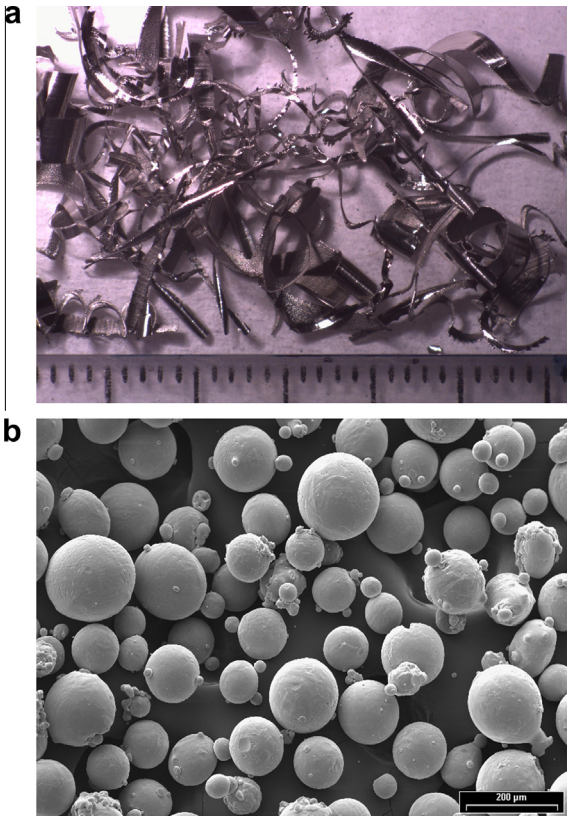

Fig. 1. (a) Tunings of Zircaloy-4 (minor division = 1 mm). (b) SEM micrograph of the Ti powders.

Morphological and chemical analyses of the samples were performed by Scanning Electron Microscopy (SEM 515, Philips Electronic Instruments) equipped with energy dispersive spectrometer (EDS). Temperature-programmed desorption (TPD) profiles were recorded in a flow system equipped with a thermal conductivity detector (Autochem II, Chemisorption Analyzer, Micromeritics). The profiles were obtained by heating the sample from rt (30 min) to 900 °C in Ar, with a heating rate of 5 °C min^{-1} and a flow rate of 40 cm^3 min^{-1}. Typically 0.2 g of sample were employed, placed in U-shaped quartz reactor and supported on quartz wool. An additional layer of quartz wool was added on top to ensure thermal homogeneity of the gas passing over the sample. After TPD, the samples were cooled under Ar flow up to rt, closed under argon atmosphere in the U-shaped reactor and transported under argon inside the glove box.

3. Results and discussion

In an attempt to produce a Zr-based alloy from zircaloy tunings and Ti powders, the milling of Zr–Ti and Zr–2Ti mixtures was performed under argon, without using a control agent. Two hours of MA were enough to completely cold weld the mixture components. It was practically impossible to recover the final powders from the milling chamber. The predominance of the cold welding process over the fracturing process in these two ductile metals is responsible for this behavior. Although the modification of process parameters might reduce the contribution of the cold welding mechanism, previous studies [14,15] have indicated the necessity of using a control agent. This evidence suggests that one powerful alternative to avoid cold welding is to modify the ductile–ductile nature of the starting mixture. In the following section, it will be shown that RMA is an excellent option to produce a Zr-based alloy due to the possibility of changing from ductile metals to brittle hydrides.

3.1. Hydriding of zircaloy tunings and Ti powders

Due to the high affinity of Zr for oxygen, the spontaneous oxidation of the tunings occurs during their formation. Different factors influence the characteristics of the oxide layer (ZrO_2) on the tuning, such as the temperature and the mechanical deformation introduced in the material during machining. To analyze the effect of the oxide layer on the zircaloy reactivity with hydrogen, we consider the thermodynamic stability of ZrO_2 in the presence of hydrogen. ZrO_2 is a very stable oxide and its reaction with hydrogen can be represented as follows:

$$ZrO_2\,(s) + 3H_2\,(g) = ZrH_2\,(s) + 2H_2O\,(g) \quad (1)$$

The standard Gibbs free-energy change (ΔG°) of reaction (1) is very positive in the temperature range between 100 and 900 °C, with values ranging from 457 to 503 kJ/mol Zr [17]. Then, the high thermodynamic stability of ZrO_2 should make zircaloy very resistant to hydrogen absorption. However, if the Zry chip surface is free of the ZrO_2 layer, its reactivity with hydrogen can be analyzed by hydriding the main constituent:

$$Zr\,(s) + H_2\,(g) = ZrH_2\,(s) \quad (2)$$

For reaction (2), ΔG° values vary from −121 to −9 kJ/mol Zr, between 100 to 900 °C, respectively [17]. A similar hydriding reaction is expected for Ti powders:

$$Ti\,(s) + H_2\,(g) = TiH_2\,(s) \quad (3)$$

where ΔG° values change from –95 to 18 kJ/mol Ti, between 100 to 900 °C, respectively.

The negative ΔG° values obtained at low temperatures indicate that hydriding both Zr and Ti is possible. However, the behavior observed during hydriding evidences different reactivity of the starting materials. Fig. 2 shows the amount of hydrogen absorbed as a function of the temperature for zircaloy tunings and titanium powders. Although titanium powders are hydrided from 370 °C, hydriding of zircaloy chips is practically undetectable after 1 h at 400 °C under 0.5 MPa of hydrogen pressure. Then, temperatures higher than 400 °C are necessary to destroy the integrity of the Zr oxide layer. Moreover, the other metals contained in Zry chips, such as Sn, Cr and Fe, do not form hydride phases under these experimental conditions. In the case of Ti, the hydriding reaction is partial (3.2 wt%) and represents about 80% of the theoretical value. A previous work [18] demonstrated the relevance of the activation process for Ti powder samples, which did not show the maximum hydrogen uptake on the first absorption/desorption cycle. The main reason of this behavior was attributed to the formation of a passivation layer on the surface that hinders hydride formation. Repetitive heat treatment under high vacuum removes this surface passivation layer, exposing fresh metal surfaces for hydrogen absorption [18].

In this context, reactive mechanical alloying (RMA) emerges as an excellent alternative to help the hydriding reaction, because it is known that it favors the reaction between metallic powders and hydrogen by creation of new free surface of the oxide layer. Fig. 3 shows the evolution of X-ray diffraction patterns of the Zr–Ti mixture as a function of milling time. The ZrH_2 and $TiH_{1.97}$ are formed in only 1 h of milling. No clear diffraction peaks from Zr and Ti (hcp or bcc) are detected. The main hydrogen consumption occurred during the first hour, as shown by the reduction of the hydrogen pressure inside the chamber. Additional milling does not show significant hydrogen pressure modification. The half height width of the most intense peaks of ZrH_2 and $TiH_{1.97}$ increases with milling time, indicating that their crystallite size decreases. For both hydrides, the crystallite size changes from 14 nm (1 h of milling) to about 7 nm (10 h of milling). The appearance of $2\theta = 43.7^\circ$ and $2\theta = 44.6^\circ$ diffraction peaks associated with Cr and Fe phases is observed since 10 h of milling time, due to the contamination with the milling chamber and balls. Moreover, after 15 h of milling, broad peaks from the fcc (Zr,Ti)H_2 phase are clearly identified. The same structure was observed during the mechanical milling of $Ti_{50}Zr_{50}$ powders in an Ar (1.8 MPa)–H_2 (0.2 MPa) atmosphere [19]. Then, at 30 h of milling, ZrH_2 and $TiH_{1.97}$ phases coexist with fcc (Zr,Ti)H_2. This phase has a crystallite size of about 4 nm, with a cell parameter $a = 0.465$ nm. Considering Fig. 2, in which hydriding was performed under 0.5 MPa up to 400 °C, the results of Fig. 3 demonstrate the efficiency of RMA for hydriding Zry and Ti under 0.5 MPa of hydrogen pressure at rt *via* the creation of new and clean surfaces. RMA of Zr–Ti mixtures generate a strong reduction in the agglomerate size in comparison with the starting material (Fig. 1a). In addition, milling under hydrogen avoids the cold working phenomena previously observed during MA of Zry and Ti without control agent, due to the change in the nature of the powders from ductile to brittle.

In a similar way, the RMA was performed for the Zr–2Ti mixture. The X-ray diffraction patterns obtained after 1 h and 5 h of milling are shown in Fig. 4. The individual hydrides of Zr and Ti are produced in only 1 h of milling. The extension of milling time induces a refinement of the microstructure: the crystallite size is reduced from 13 nm (9 nm) to 11 nm (7 nm) for ZrH_2 ($TiH_{1.97}$). In addition, the appearance of a solid–solution phase type (Zr–Ti)H_2

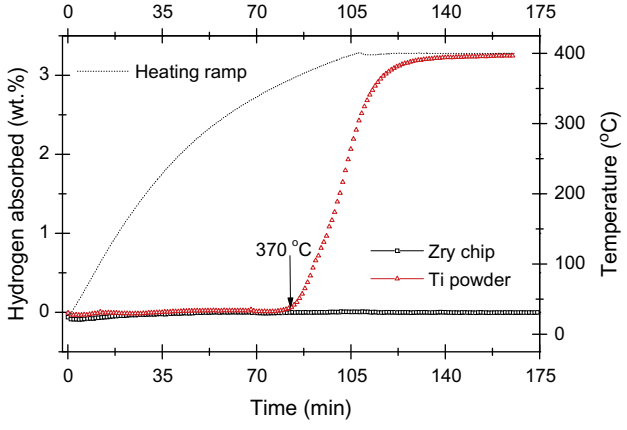

Fig. 2. Non-isothermal hydriding of Zr tunings and Ti powders. Hydrogen absorption was performed using about 5 °C min^{-1} heating rate to a final temperature of 400 °C under 0.5 MPa of hydrogen.

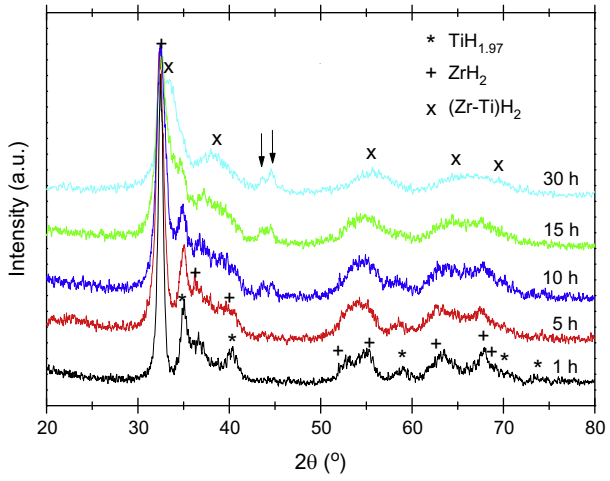

Fig. 3. X-ray diffraction patterns of the Zr–Ti mixture after different milling times. RMA was performed under 0.5 MPa of hydrogen at room temperature.

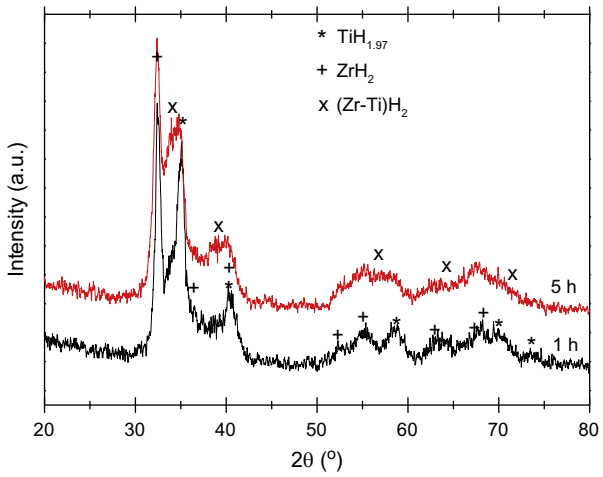

Fig. 4. X-ray diffraction patterns of the Zr–2Ti mixture after different milling times. RMA was performed under 0.5 MPa of hydrogen at room temperature.

is detected after 5 h of milling, simultaneously with ZrH_2 and $TiH_{1.97}$ phases. Then, RMA of Zr and Ti powders under hydrogen atmosphere lead to the formation of ZrH_2 and $TiH_{1.97}$ and the simultaneous formation of nanocrystalline $(Zr–Ti)H_2$. Based on the results showed after RMA of the Zr:Ti mixture (Fig. 3) and to avoid the starting material contamination from both vial and balls of milling, additional milling for more than 5 h was not performed. As it will be shown in the next Section 3.2, the RMA for 5 h is enough to ensure the further formation of Zr–2Ti alloy by heating under argon up to 900 °C. As a possible alternative to avoid contamination, RMA could be performed using wear-resistant milling vial and balls.

The microstructure of the powders after RMA was studied by SEM. Fig. 5a shows the agglomerate size distribution for Zr–Ti mixtures after 5 h of milling. From this figure it can be seen that the particles have irregular shapes and sizes, with a wide agglomerate size distribution from 20 to 400 μm. Fig. 5b shows a detail of the agglomerate surface, which looks fluffy and granular showing an increment in the powder surface area with respect to the starting materials (Fig. 1). Similar shape and agglomerate size distribution were observed for the Zr–2Ti mixture after 5 h of RMA. From EDS analyses, the average values of Zr, Ti and the minor component of Zry alloy were obtained. The atomic ratio between Zr and Ti is in agreement with the nominal atomic relation for both starting mixtures after 5 h of milling. The content of the other metals (Sn + Fe + Cr) is <4 at.%. This result demonstrates the homogeneous distribution of Zr and Ti in the milled samples. Then, the RMA process promotes a reduction of agglomerate size (Fig. 5a), an increase of surface area (Fig. 5b) and a uniform distribution of phases. These microstructural modifications were reached during metal hydride formation due to an adequate balance between both cold welding and fracturing processes, even without the use of a control agent.

3.2. Decomposition of the hydride phases by thermal treatment

To produce the Zr-based alloy from both Zr:Ti compositions, the hydrided samples by RMA (Figs. 3 and 4) were heated up to 900 °C under a constant flow of Ar, using a ramp of 5 °C min^{-1}. This temperature was selected on the basis of decomposition temperature reported for each hydride, to ensure complete hydrogen release [18,20–23]. The hydrogen desorption behavior of the Zr:Ti mixtures after different milling times was assessed using TPD profiles (Fig. 6). All as-milled Zr–Ti mixtures released hydrogen in a two-stage desorption process, with maxima at approximately

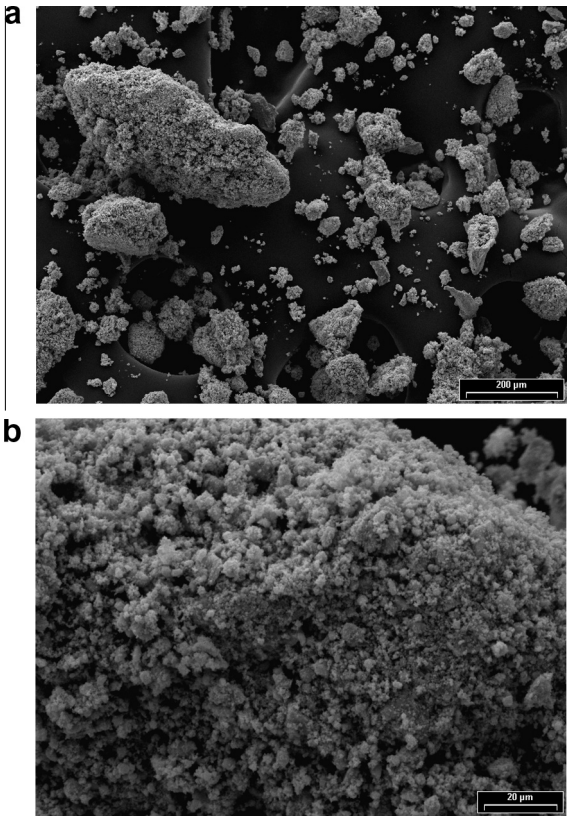

Fig. 5. (a) Wide area of SEM micrograph for the Zr–Ti mixture after 5 h of RMA. (b) Agglomerate surface detail.

520 °C and 730 °C after 5 h of milling. This two-stage behavior could be attributed to the decomposition of $TiH_{1.97}$ (stage 1) [18,20,21], followed by the decomposition of ZrH_2 (stage 2) [22,23]. For both Zr:Ti mixtures, the onset desorption temperature of the TPD profiles is shifted by more than 200 °C as milling time increases from 1 h to 5 h. In addition, while the decomposition temperature of $TiH_{1.97}$ slightly changes with the milling time and the composition of the starting mixture, the peak position corresponding to the ZrH_2

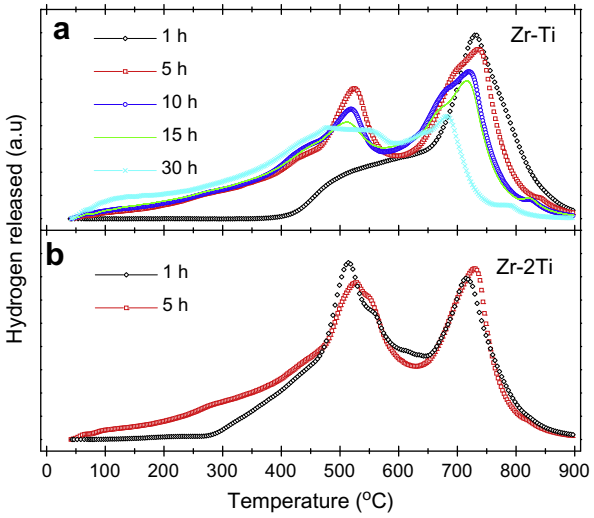

Fig. 6. TPD profiles for the Zr–Ti mixtures after RMA: (a) Composition 1:1 after 1, 5, 10, 15 and 30 h. (b) Composition 1:2 after 1 and 5 h. Experiments were performed using a 5 °C min^{-1} heating rate to a final temperature of 900 °C under 40 cm^3 min^{-1} Ar gas flow.

decomposition clearly shifts to lower temperatures for the Zr:Ti composition from 10 to 30 h of milling (Fig. 6). The decrease in the onset temperature of hydrogen desorption could be associated with the microstructural modifications (reduction of agglomerate size, increase of surface area, reduction in the crystallite size) introduced in the material as the milling time increases (§1.2, Figs. 3–5). The shape of TPD profiles suggests that the milling time has a stronger effect on the ZrH_2 microstructure and then on its decomposition (second stage). For all TPD profiles, the decomposition of the hydride phases was completed. In this way, during hydrogen release, clean Ti and Zr metallic surfaces are generated *in situ* and the alloy formation could be favored when the metals are homogeneously distributed and in good contact.

Thus, to investigate if thermal treatment up to 900 °C under Ar is enough to favor the formation of Zr–Ti alloys, the final materials were characterized using XRPD and SEM. Figs. 7a and 7b shows the diffraction patterns obtained at the end of the TPD profile for the Zr–Ti ratio of 1:1 and 1:2, respectively. The results indicate that crystal structure of the final Zr alloys is sensitive to the extension of the milling time previous to the thermal treatment. As shown in Figs. 7a and 7b for the both compositions, 5 h of RMA followed by thermal treatment successfully leads to the formation of the β phase. The β phase is metastable at room temperature and retained during cooling [4]. The estimated lattice parameters are $a = 0.344$ nm and $a = 0.339$ nm for the Zr:Ti ratio of 1:1 and 1:2, respectively. The crystallite size calculated for both compositions is about 30 nm, confirming the nanostructure of the final powders. Since the atomic radius of Ti (1.47 Å) is smaller than that of Zr (1.62 Å), the addition of Ti caused the shift toward a high angle value for Zr:2Ti composition, which reflects the higher content of Ti in the final β alloy and a smaller cell parameter. However, after 1 h of milling the final phases obtained reflect the incomplete degree of mixing between Zr and Ti. On the one hand, in the case of Zr–Ti composition, a mixture of α (∼70 at.% Zr) and β (∼50 at.% Zr) phases is produced. On the other hand, for the Zr–2Ti composition, free Ti and α (∼70 at.%Zr) phases are detected simultaneously with the β (∼33 at.% Zr) phase. Then, RMA for 1 h is not enough to ensure the nominal composition homogenously distributed in the sample.

The final microstructure of the β phase obtained after RMA during 5 h, followed by thermal treatment for 1:1 and 1:2 Zr–Ti compositions, was characterized by SEM (Figs. 8a and 8b). As it can be seen from this figure, the collected powders were fully metallized into a well-consolidated porous structure. The surface looks like

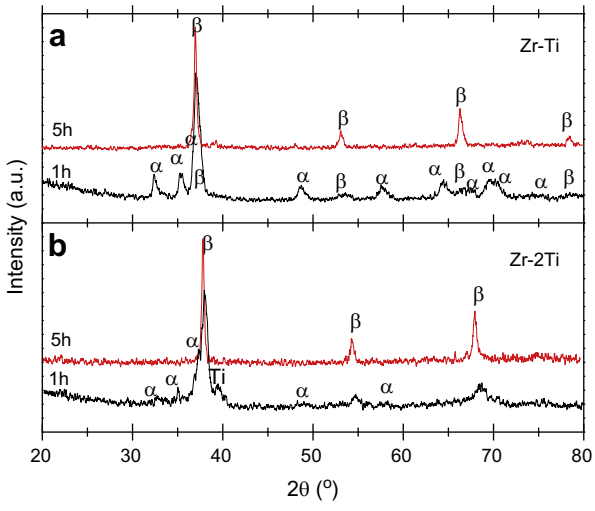

Fig. 7. X-ray diffraction patterns of the Zr–Ti mixture after RMA and subsequent thermal treatment up to 900 °C (heating ramp of 5 °C min^{-1}). (a) Composition 1:1. (b) Composition 1:2.

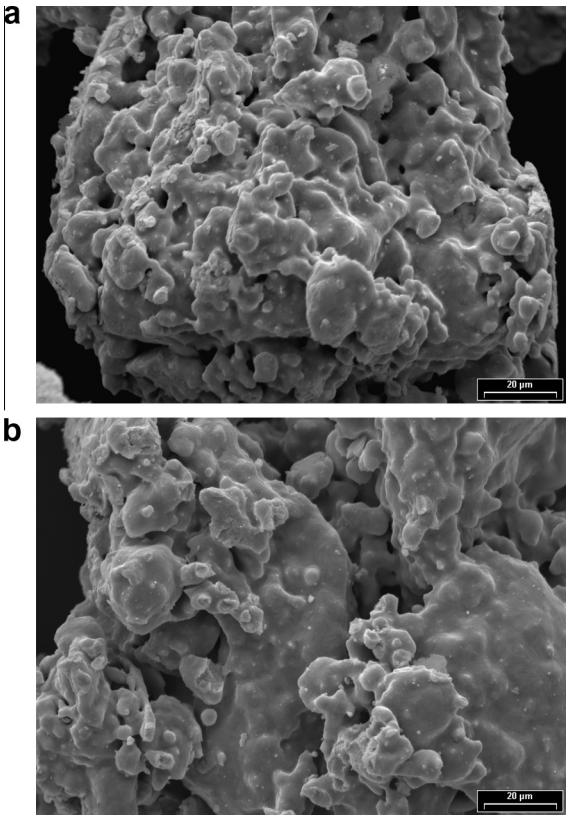

Fig. 8. Surface detail of the Zr–Ti solid solution powders after thermal treatment up to 900 °C. (a) Composition 1:1; (b) Composition 1:2.

interconnected particles with irregular forms. Different EDS analyses present a homogeneous distribution of Zr and Ti in all milled samples, in agreement with the nominal Zr:Ti ratio. Then, it is clearly shown that 5 h of RMA process are necessary to favor the homogeneous Zr and Ti distribution. Further thermal treatment under argon flow up to 900 °C is enough to produce the β phase. Consequently, the synthesis of Zr-based alloys of different composition was achieved by combination of RMA at rt for a selected time and posterior thermal treatment of Zr–Ti hydrided mixtures at only 900 °C. Therefore, the method developed here for alloy production requires lower temperatures than the traditional melting process. The experimental evidence suggests that the method proposed for the production of Zr-based alloys could be extended to other metals different from Ti.

4. Conclusions

In this work, zircaloy tunings were used as a valuable source of Zr for the production of Zr–Ti alloys. The bcc β alloys, with different compositions, were successfully produced by a two-step process.

During the first step, mixtures of zircaloy tunings and Ti powders were RMA at room temperature and without a control agent. The formation of ZrH_2 and $TiH_{1.97}$ was observed after 1 h of milling for both Zr–Ti compositions. Experimental evidence demonstrated that the RMA process promotes the size reduction of agglomerates, the increase of surface area and the uniform distribution of the hydrided phases after 5 h of milling. The material embrittlement, that occurs during RMA, allows both a balance between cold working and fracturing process and the progress of MA without the use of a control agent.

In the second step, the hydrided phases were decomposed by the thermal treatment up to 900 °C under argon flow. Hydrogen

was released in a two-stage desorption process, with maxima at about 520 °C and 730 °C attributed to the decomposition of $TiH_{1.97}$ and ZrH_2, respectively. It was demonstrated that the first step of RMA has to be performed for more than 1 h to produce a homogeneous solid solution. The as-produced alloys were in well-consolidated porous structures. The findings presented in this paper can lead to a generic approach for the synthesis of other Zr-based alloys.

Acknowledgments

This study has been partially supported by CONICET (National Council of Scientific and Technological Research), CNEA (National Atomic Energy Commission), ANPCyT, Instituto Balseiro-UNC (University of Cuyo) and UNL (University of Litoral). One of the authors (N.S. Gamba) wishes to thank the financial support of Inter-U (Exchange Program between National Universities) during her stay at Instituto Balseiro (University of Cuyo). Thanks are given to Elsa Grimaldi for the English language editing.

References

[1] B. Lustran, F. Kerze, The metallurgy of Zirconium, McGraw-Hill, New Cork, 1995. pp. 19.
[2] H.M. Grandin, S. Berner, M. Dard, A review of titanium zirconium (TiZr) alloys for use in endosseous dental implants, Materials 5 (2012) 1348–1360.
[3] N. Stojilovic, E.T. Bender, R.D. Ramsier, Surface chemistry of zirconium, Prog. Surf. Sci. 78 (2005) 101–184.
[4] J.L. Murray, Binary alloy phase diagrams, in: H. Baker (Ed.), Alloys Phase Diagrams, ASM International, Materials Park, OH, 1987, p. 340.
[5] W.-F. Ho, W.-K. Chen, S.-C. Wu, H.-C. Hsu, Structure, mechanical properties and grindability of dental Ti–Zr alloys, J. Mater. Sci.: Mater. Med. 19 (2008) 3179–3186.
[6] M. Takahashi, M. Kikuchi, O. Okino, Grindability of dental cast Ti–Zr alloys, Mater. Trans. Jpn. 50 (2009) 859–863.
[7] W.F. Ho, C.H. Cheng, C.H. Pan, S.C. Wu, H.C. Hsu, Structure, mechanical properties and grindability of dental Ti–10Zr–X alloys, Mater. Sci. Eng. C 29 (2009) 36–43.
[8] H.C. Hsua, S.C. Wua, S.K. Hsua, Y.C. Sung, W.F. Ho, Effects of heat treatments on the structure and mechanical properties of Zr–30Ti alloys, Mater. Charact. 62 (2011) 157–163.
[9] H.C. Hsu, S.C. Wu, Y. C Sung, W.F. Ho, The structure and mechanical properties of as-cast Zr–Ti alloys, J. Alloys Comp. 488 (2009) 279–283.
[10] O. Okuno, A. Shimizu, I. Miura, Fundamental study on titanium alloys for dental casting, J. Jpn. Soc. Dent. Mat. Dev. 4 (1985) 708–715.
[11] C. Suryanarayana, Mechanical Alloying and Milling, Marcel Dekker, New York, 2004. pp. 183.
[12] K. Aoki, A. Memezawa, T. Masumoto, Nitrogen-induced amorphization of Ti-Zr powders during mechanical alloying, Appl. Phys. Lett. 61 (1992) 1037–1039.
[13] K. Aoki, A. Memezawa, T. Masumoto, Amorphization of Ti–Zr powders by mechanical alloying in H_2, N_2 and O_2 atmospheres, Mater. Sci. Eng. A 181 (1994) 1263–1267.
[14] S. Wang, S. Li, B. Xu, F. Cai, L. Li, J. Lei, J. Alloys Comp. 429 (2007) 227–232.
[15] C.E. Wen, Y. Yamada, P.D. Hodgson, Fabrication of novel TiZr alloy foams for biomedical applications, Mater. Sci. Eng. C 26 (2006) 1439–1444.
[16] A.J. Parkison, S.M. McDeavitt, Hydride formation process for the powder metallurgical recycle of zircaloy from used nuclear fuel, Metall. Mater. Trans. A 42A (2011) 192–201.
[17] Outokumpu HSC Chemistry for Windows, version 6.1; Outokumpu Research Oy, Finland, 2009.
[18] J.L. Blackburn, P.A. Parilla, T. Gennett, K.E. Hurst, A.C. Dillon, Michael J. Heben, Measurement of the reversible hydrogen storage capacity of milligram Ti–6Al–4V alloy samples with temperature programmed desorption and volumetric techniques, J. Alloys Comp. 454 (2008) 483–490.
[19] A. Memezawa, K. Aoki, T. Masumoto, Amorphization of Ti-Zr powders by the collaborated interaction of mechanical alloying and hydrogenation, Scr. Mater. 28 (1993) 361–365.
[20] J.F. Fernández, F. Cuevas, C. Sanchez, Simultaneous differential calorimetry and thermal desorption spectroscopy measurements for the study of the decomposition of metal hydrides, J. Alloys Comp. 298 (2000) 244–253.
[21] S. Morosova, T.I. Khomenko, Ch. Porchers, A.V. Leonov, Effect of mechanically induced modification on TiH_2 thermal stability, J. Alloys Comp. 509 (2011) S754–S758.
[22] F. von Zeppelin, M. Hirscher, H. Stanzick, J. Banchart, Compos. Sci. Technol. 63 (2003) 2293–2300.
[23] W. Chen, L. Wang, S. Lu, Influence of oxide layer on hydrogen desorption from zirconium hydride, J. Alloys Comp. 469 (2009) 142–145.